Cell Stem Cell, volume *11*

Supplemental Information

Coordination of Satellite Cell Activation and Self-Renewal by Par-Complex-Dependent Asymmetric Activation of p38α/β MAPK

Andrew Troy, Adam B. Cadwallader, Yuri Fedorov, Kristina Tyner, Kathleen Kelly Tanaka, and Bradley B. Olwin

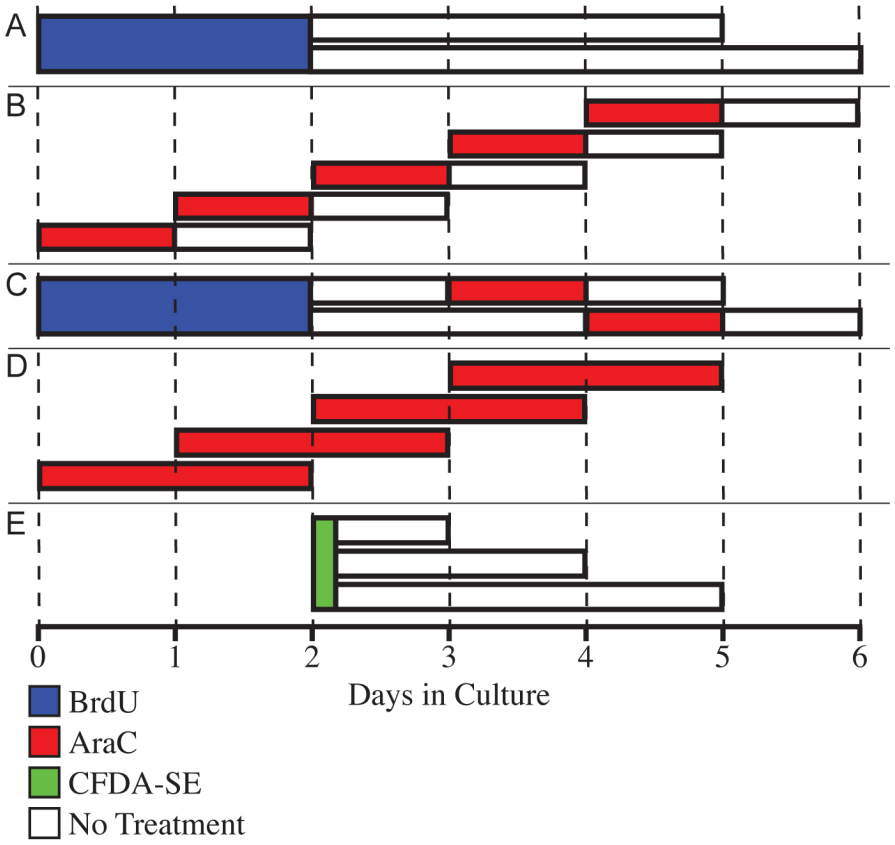

Figure S1. BrdU, AraC and CFDA-SE treatment of myofiber-associated and dispersed satellite cell cultures, related to Figures 1 and 2. A diagram illustrating the BrdU (A, C), AraC (B-D) and CFDA-SE (E) treatment time courses of myofiber-associated and dispersed satellite cell cultures for Figures 1 and 2.

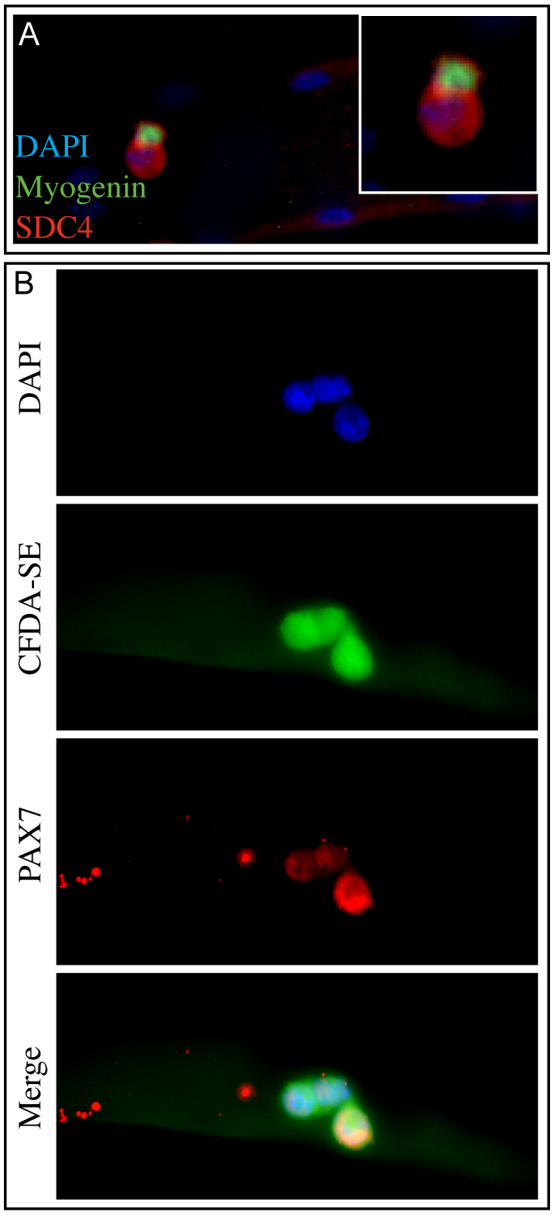

Figure S2. A subset of satellite cells becomes quiescent after one division, related to Figure 2. Myogenin+ cells are terminally differentiated and thus, are AraC-resistant and present when myofiber cultures are AraC treated from 3d-5d (A). CFDA-SE labels all satellite cells (B, PAX7, red) when myofibers cultured for 2d were treated with CFDA-SE (B, green) for 15 min and fixed 30 min later (B).

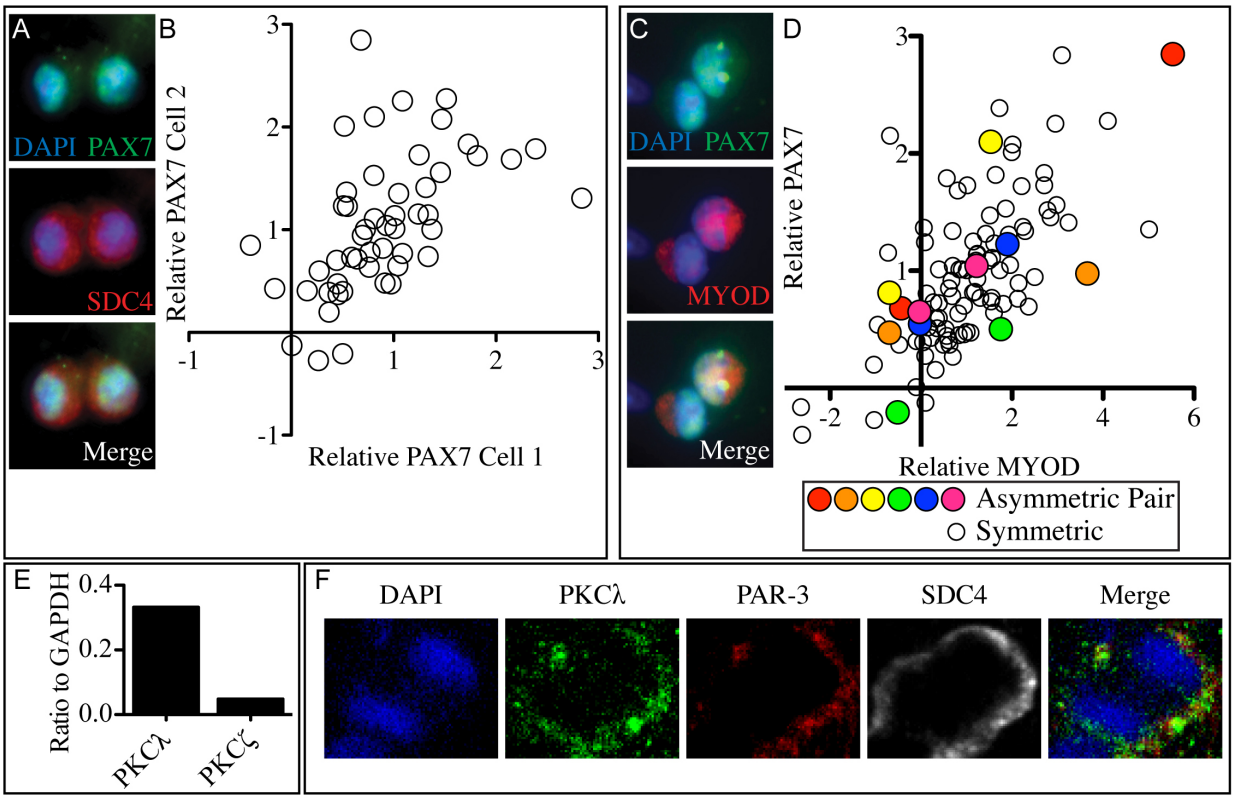

Figure S3. Satellite cells do not asymmetrically distribute PAX7, related to Figure 3. All Syndecan-4+ (A, red) cell pairs have equivalent levels of nuclear PAX7 immunofluorescence (A, green) at 48h (A, B). Each circle indicates an individual pair of daughter cells and each axis indicates relative nuclear PAX7 fluorescence intensity above cytoplasmic background in one cell of the pair (B). Daughter cell pairs with asymmetric MYOD (C, red) do not exhibit asymmetric PAX7 immunofluorescence (C, green; D). Each circle represents an individual cell in a SDC4+ cell pair (D). For each cell the relative nuclear MYOD fluorescence intensity is plotted on the X-axis and the relative nuclear PAX7 fluorescence intensity is plotted on the Y-axis (D). Colored circles mark 6 daughter pairs with asymmetric MYOD immunofluorescence where both daughter cells of each pair are marked with the same color (C; red, orange, yellow, green, blue, purple) and empty smaller circles indicate cells in daughter pairs with symmetric MYOD (D). *Pkcλ*

transcripts are detected at 7-fold higher levels than *Pkcζ* transcripts in satellite cells isolated 48h following injury as measured by qPCR (E). Asymmetric PAR-3 and PKCλ co-localize in dividing satellite cells on myofibers cultured for 36h (F). Note that both are anti-rabbit antibodies and this prevented routine staining and scoring in our experiments.

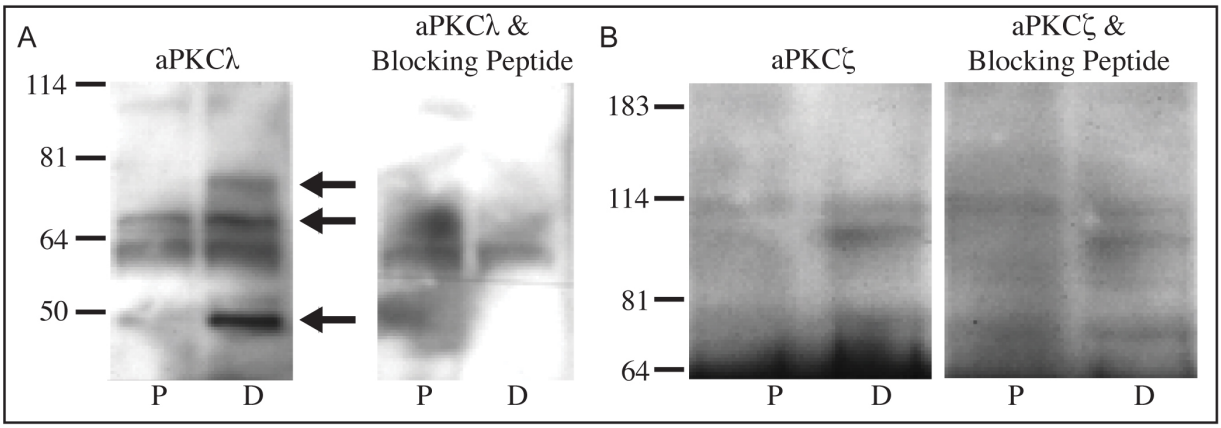

Figure S4. MM14 cells express PKCλ but not PKCζ, related to Figure 4. PKCλ (A), but not PKCζ (B), is detected by Western blot in MM14 cells grown under proliferating (P) or differentiating (D) conditions for 48 hours. Cell lysates were probed with anti-PKCλ antibodies (A) or anti-PKCζ antibodies (B) by Western blot in the presence or absence of the respective specific blocking peptide. Black arrowheads denote PKCλ-specific proteins.

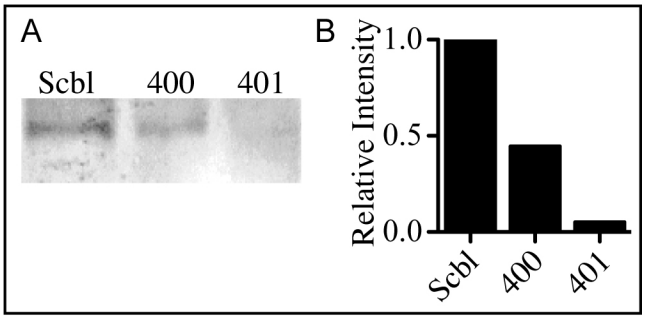

Figure S5. Expression of shRNAs targeting *Par-3* transcripts reduces PAR-3 protein levels.

Transfection of plasmids expressing shRNAs to *Par-3* (400 and 401) reduces *Par-3* protein levels by 2-fold and 20-fold in FACS enriched NIH-3T3 cells, respectively compared to cells transfected with a plasmid expressing a scrambled shRNA (Scbl) as shown by Western blot (A, B). The relative intensity of the PAR-3 proteins were normalized to Ponceau staining (B).

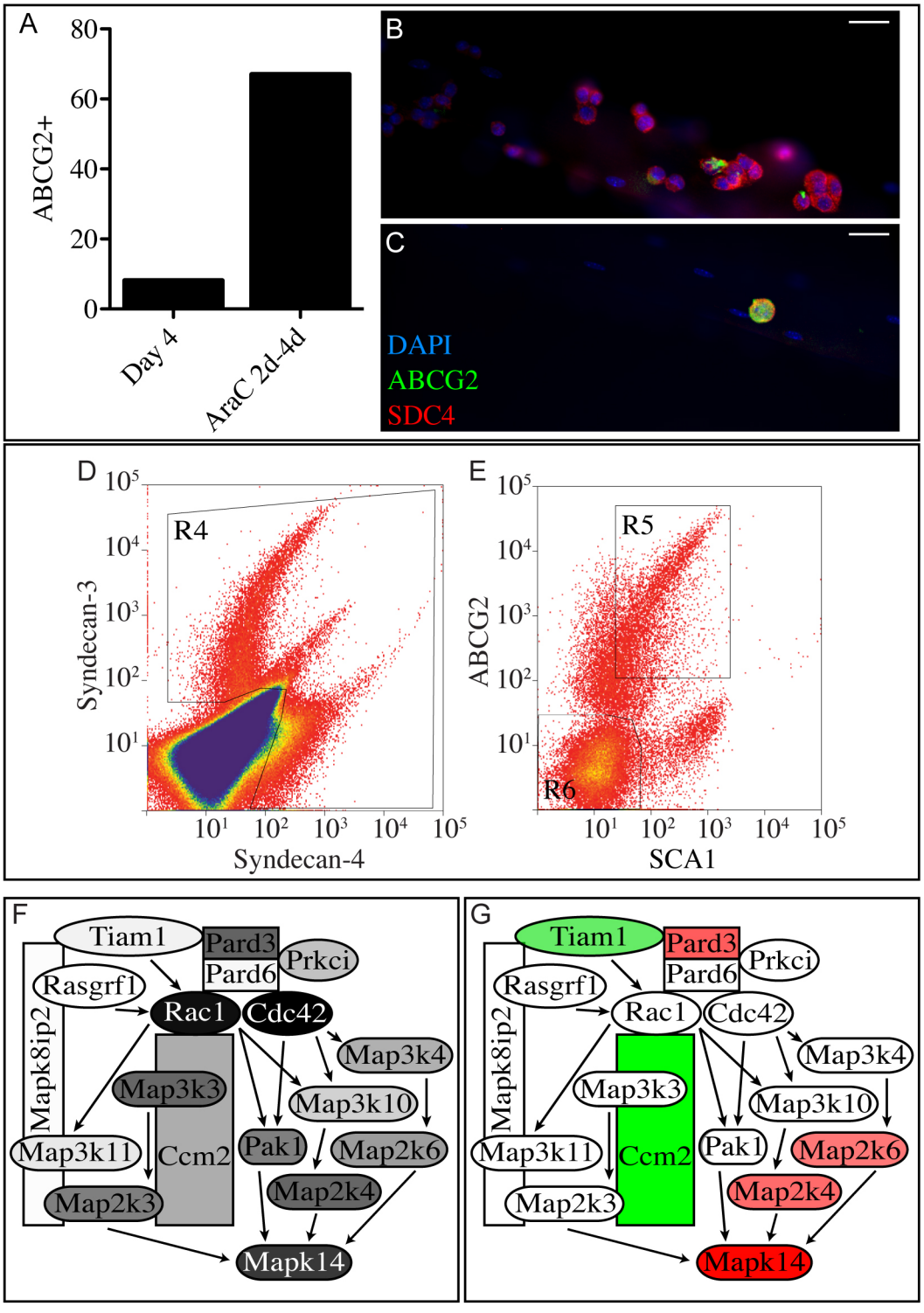
A
80
60
40
20
0
ABCG2+
Day 4
AraC 2d-4d
B
C
DAPI
ABCG2
SDC4
D
R4
Syndecan-3
Syndecan-4
E
R5
R6
ABCG2
SCA1
F
Tiam1
Pard3
Pard6
Prkci
Rasgrf1
Rac1
Cdc42
Mapk8ip2
Map3k4
Map3k3
Map3k10
Map3k11
Ccm2
Pak1
Map2k6
Map2k3
Map2k4
Mapk14
G
Tiam1
Pard3
Pard6
Prkci
Rasgrf1
Rac1
Cdc42
Mapk8ip2
Map3k4
Map3k3
Map3k10
Map3k11
Ccm2
Pak1
Map2k6
Map2k3
Map2k4
Mapk14

Figure S6. Satellite-SP cells and satellite cells exhibit distinct gene expression profiles for Par complex-p38α/β MAPK signaling components, related to Figure 7. AraC-resistant syndecan-4+, myofiber-associated cells, treated from 2d to 4d of culture are enriched 8-fold for ABCG2, a satellite-SP cell marker (A, C)(Tanaka et al., 2009) compared to cells on untreated myofibers at 4d (A, B). Syndecan-4+/Syndecan-3+ satellite cells were enriched by FACS (D, E, R4) and separated from satellite-SP cells expressing SCA1 and ABCG2 (D, E, R5), RNA isolated and gene expression profiles determined using Affymetrix 430A gene chip arrays. Signaling pathways linking the Par complex to *p38αmapk* were constructed using Ingenuity Pathway analysis and literature searches. Overlaying Affymetrix gene chip array on these putative pathways allows visualization of the expression of genes potentially involved in the regulation of *p38α mapk* by the Par complex in satellite cells (F, see Table S1) and the differential gene expression between satellite cells and satellite-SP cells (G, see Table S2). The diagram (F) depicts relative gene expression values for the satellite cell population devoid of satellite-SP cells (F, the level of gray intensity indicates relative gene expression values with black highest). The diagram (G) illustrates differences in relative gene expression of 2-fold or greater ($p \leq 0.02$) between satellite-SP cells (G, green) and satellite cells (G, red). The intensity of green or red color indicates the relative difference in gene expression levels where white is less than a 2-fold change or no significant difference between satellite and satellite-SP cells, green is higher relative expression in satellite-SP cells and red is higher relative expression in satellite cells (see Table S2). Each gene is identified by the GenBank *mus musculus* gene name.

Table S1. Protein interactions, related to Figure 7. Signaling networks linking the Par complex to p38α/β MAPK signaling were derived by literatures searches combined with

Ingenuity Pathway Analysis. The proteins implicated, the nature of their interaction and references to the articles where the protein interactions are described are listed. These putative signaling pathways are illustrated in Figures 7E and F.

Table S2. Differential gene expression by satellite cells and satellite-SP cells in a putative Par complex/p38α/β MAPK signaling network, related to Figure 7. The gene symbol, probeset ID, gene expression values for satellite cells devoid of the satellite-SP population (log_2), the fold-change relative to the satellite-SP population and the associated p-value is listed for each gene depicted in Figure 7E, F. Red and green coloring indicates a fold change of 2-fold or greater and a p-value < 0.02.

Movie S1. PAR-3 and phospho-p38α/β MAPK are present in an asymmetric complex during the first division following isolation of dispersed satellite cells, related to Figure 6. Primary satellite cells were isolated and cultured for 36h as described in Experimental Procedures. Mitotic (phospho-Histone 3, blue) satellite cells (*Pax7*$^{tmLacZ/+}$ βgal, red) were probed for complexes containing PAR-3 and pp38α/β MAPK by PLA (green). The movie displays a 3D confocal reconstruction of a mitotic satellite cell, demonstrating that complexes containing Par-3 and phospho-p38α/β MAPK are localized to the edges of the cell and the surface in contact with the substrate contact surface. A graph quantifying the total number of complexes per mitotic satellite cell is shown in Figure 6.

Movie S2. SCA1 and phospho-p38α/β MAPK are asymmetrically localized to opposite prospective daughter cells during division, related to Figure 7. Myofibers were

isolated and cultured for 36h as described in Experimental Procedures. A movie of a 3D confocal reconstruction shows a dividing, myofiber-associated satellite cell (Syndecan-4, white) probed for SCA1 (red) and phospho-p38α/β MAPK (green) where SCA1 and phospho-p38α/β MAPK are localized to opposite prospective daughter cells.

Table S1

Protein	Protein	Interaction	Reference
PARD3	PARD6	Binding via PDZ domains	(Lin et al., 2000)
PARD3	PRKCI	Binding via PRKCI regulatory domain	(Joberty et al., 2000)
PARD3	TIAM1	Binding via TSS region and negative regulation of RAC-GEF activity	(Chen and Macara, 2005; Nishimura et al., 2005)
CDC42	PRKCI	Positive regulation via PARD6 binding	(Yamanaka et al., 2001)
PARD6	PRKCI	Binding via PRKCI regulatory domain	(Joberty et al., 2000)
PARD6	RAC1	Binding via PARD6 CRIB motif	(Lin et al., 2000)
PARD6	CDC42	Binding via PARD6 CRIB motif	(Lin et al., 2000)
TIAM1	RAC1	Activation of RAC1 via GEF activity	(van Leeuwen et al., 1995)
TIAM1	MAP3K11	TIAM1 binding to MAPK8IP2 increases binding of MAP3K11 to MAPK8IP2	(Buchsbaum et al., 2002)
TIAM1	MAP2K3	TIAM1 binding to MAPK8IP2 increases binding of MAP2K3 to MAPK8IP2	(Buchsbaum et al., 2002)
TIAM1	MAPK14	TIAM1 binding to MAPK8IP2 increases binding of MAPK14 to MAPK8IP2	(Buchsbaum et al., 2002)
MAPK8IP2	TIAM1	Binding via TIAM1 PH-CC-Ex region	(Buchsbaum et al., 2002)
MAPK8IP2	RASGRF1	Binding via RASGRF1 PH-CC-Ex region	(Buchsbaum et al., 2002)
MAPK8IP2	MAP3K11	Binding via MAPK8IP2 C-terminal region; increased MAP3K11 activity when MAPK8IP2 over-expressed with TIAM1	(Buchsbaum et al., 2002)
MAPK8IP2	MAP2K3	Binding via MAPK8IP2 amino acids 511 to 835	(Buchsbaum et al., 2002)
MAPK8IP2	MAPK14	Binding via MAPK8IP2 amino acids 1 to 306; increased MAPK14 activity when MAPK8IP2 over-expressed with TIAM1	(Buchsbaum et al., 2002)
RASGRF1	RAC1	Activation of RAC1 via GEF activity	(Innocenti et al., 1999)
RAC1	MAP3K11	Activation of MAP3K11, binding via MAP3K11 CRIB motif and increase MAP3K11 binding to MAPK8IP2	(Nagata et al., 1998; Lambert et al., 2002; Buchsbaum et al., 2002)
RAC1	MAP2K3	Increase MAP2K3 binding to MAPK8IP2	(Buchsbaum et al., 2002)
RAC1	PAK1	Binds and activates PAK1 via autophosphorylation	(Manser et al., 1994)
RAC1	MAP3K10	Binding via MAP3K10 CRIB motif	(Nagata et al., 1998)
CDC42	PAK1	Binds and activates PAK1 via autophophorylation	(Manser et al., 1994)
CDC42	MAP3K11	Activation of MAP3K11 via phosphorylation of MAP3K11 activation loop and binding via MAP3K11 CRIB motif	(Nagata et al., 1998; Du et al., 2005)
CDC42	MAP3K10	Binding via MAP3K10 CRIB Motif	(Nagata et al., 1998)
CDC42	MAP3K4	Binding; positively mediates CDC42 signaling	(Gerwins et al., 1997)
RAC1	CCM2	Binding; Regulation of MAP3K3/CCM2 dependent MAPK14 activation	(Uhlik et al., 2003)
CCM2	MAP3K3	Binding; Increased activation of MAP2K3 by MAP3K3	(Uhlik et al., 2003)

CCM2	MAP2K3	Binding; Increased activation of MAP2K3 by MAP3K3	(Uhlik et al., 2003)
MAP3K3	MAP2K3	Phosphorylation and activation of MAP2K3	(Deacon and Blank, 1997)
MAP3K10	MAP2K4	Phosphorylation and activation of MAP2K4	(Hirai et al., 1997)
MAP3K4	MAP2K6	Phosphorylation and activation of MAP2K6	(Takekawa et al., 1997)
PAK1	MAPK14	Activation of MAPK14	(Zhang et al., 1995)
MAP2K3	MAPK14	Activation of MAPK14 by phosphorylation	(Dérijard et al., 1995)
MAP2K4	MAPK14	Activation of MAPK14 by phosphorylation	(Dérijard et al., 1995)
MAP2K6	MAPK14	Activation of MAPK14 by phosphorylation	(Raingeaud et al., 1996)

Table S2

Gene Symbol	Probeset ID	Non-SP $\log_2$ Expression	Fold Increase in SP	P-value
Pard3	1434775_at	2.49	0.09	0.000003
Pard6a	1449100_at	1.43	1.19	0.30
Pirkc	1449100_at	1.81	0.60	0.01
Tiam1	1453887_a_at	1.46	2.69	0.001
Rasgrf1	1424734_at	1.37	1.02	0.12
Rac1	1451086_s_at	3.12	0.92	0.04
Cdc42	1449574_a_at	3.22	1.39	0.008
Mapk8ip2	1418785_at	1.38	1.70	0.10
Ccm2	1434648_a_at	1.96	9.91	0.00001
Map3k11	1450669_at	1.46	1.15	0.16
Map3k3	1436522_at	2.48	0.65	0.004
Map3k10	1436373_at	1.70	1.76	0.05
Map3k4	1450253_a_at	1.95	0.81	0.14
Map2k3	1451714_a_at	2.30	0.81	0.01
Map2k4	1426850_a_at	2.48	0.16	0.0001
Map2k6	1451982_at	2.09	0.44	0.0003
Pak1	1420979_at	2.30	0.58	0.0001
Mapk14	1459617_at	2.81	0.02	0.001

Supplemental Experimental Procedures

Mice

Mice were housed in a pathogen-free facility and the Institutional Animal Care and Use Committee at the University of Colorado approved all procedures and protocols. Mice were female between 3 and 5 months of age. Wild type mice were B6D2F1 (The Jackson Laboratory) and mice carrying the *Pax7*-LacZ allele have been previously described and were provided by Dr. Michael Rudnicki (Kuang et al., 2006).

Cell Culture

To isolate primary satellite cells, hind limb skeletal muscle was dissected away from the bone and fat and connective tissue was removed. The muscle was subsequently minced with scalpels for 10 minutes and then incubated in collagenase for 1 hour. Undigested tissue was removed by centrifugation at 6 x g and the supernatant was subsequently centrifuged at 1500 x g to pellet the satellite cells. The pellet was resuspended in media containing serum and filtered sequentially through 70 μM and 40 μM filters. Cells were cultured on tissue culture dishes for 12 hours to remove adherent fibroblasts. Non-adherent cells were then transferred to gelatin-coated coverslips.

To isolate live myofibers for culture, hind limb skeletal muscle was dissected and digested for 1 hour in collagenase. The collagenase mixture was then transferred to tissue culture dishes containing serum to stop collagenase activity. Live myofibers were isolated from the mixture with a fire polished glass pipette and transferred to another tissue culture dish. The isolation of individual myofibers by pipette was repeated at least two subsequent times to ensure the removal of dead myofibers and cellular debris.

Primary satellite cells and MM14 cells were cultured on gelatin-coated coverslips while live myofibers were cultured in uncoated plastic tissue culture dishes. All cells were cultured in

F12-C (Life Science Products Inc) with 15% horse serum and 1 nM FGF-2. MM14 cells were induced to differentiate by culturing in F12-C + 5% horse serum. AraC (Sigma Aldrich) was used at 100 μM and BrdU (Sigma Aldrich) and CFDA-SE (Invitrogen) were used at 10 μM.

Immunofluorescence

For immunofluorescence analysis, cells and myofibers were fixed in 4% paraformaldehyde for 15 minutes and subsequently permeablized (when necessary) in PBS + 0.2% Triton X-100 for 30 minutes. Samples were blocked in 10% goat serum or 5% BSA for 1 hour and incubated in primary antibody in 10% goat serum or 3% BSA for 1 hour at room temperature or overnight at 4ºC. Samples were washed 5 times in PBS + 0.02% Triton X-100 and then incubated in secondary antibody for 1 hour at room temperature. Following treatment with secondary antibody, samples were washed 5 times in PBS + 0.02% Triton X-100 and mounted on slides in Vectashield or Vectashield containing DAPI.

Primary antibodies and dilutions: rat polyclonal anti-BrdU (Serotec) at 1:100, mouse monoclonal PAX7 (Developmental Hybridoma Bank at Iowa University) at 1:5, rabbit polyclonal MYOD (C-20, Santa Cruz Biotechnology) at 1:800, chicken anti-syndecan-4 (Cornelison et al., 2001) at 1:1500, mouse monoclonal anti-Myogenin (F5D, (Cusella-De Angelis et al., 1992)) at 1:3, rat monoclonal anti-pH3 (Sigma Aldrich) at 1:500, rabbit polyclonal anti-pH3 (Millipore) at 1:250, mouse monoclonal anti-ABCG2 (BCRP1) 5D3 (BD Pharmingen), rabbit polyclonal anti-PKCλ (Santa Cruz Biotechnology) at 1:50, rabbit polyclonal anti-PAR-3 (Upstate) at 1:250, rabbit polyclonal anti-ß-galactosidase (Sigma Aldrich) at 1:250, mouse monoclonal anti-myosin heavy chain (MF20) (Bader, Masaki and Fischman, 1982), chicken polyclonal anti-ß-galactosidase antibody (Abcam) at 1:500, mouse monoclonal SCA1 (BD Pharmingen) at 1:50, rabbit polyclonal anti-p38 (C-20, Santa Cruz Biotechnology) at 1:50 and

mouse monoclonal anti-phospho-p38 (Cell Signaling) at 1:50. Alexa Fluor 488, 555 and 647 conjugated secondary antibodies (Invitrogen) were used at a 1:1000 dilution.

Transfection

MM14 cells and primary satellite cells were transfected by a calcium phosphate-DNA precipitate method. 10,000 cells per well were plated in 6-well plates. A calcium phosphate-DNA precipitate was made and resuspended in HEPES-buffered saline and 2M $CaCl_2$ was added slowly to a concentration of 110 mM while vortexing. DNA was allowed to precipitate for 20 minutes at room temperature. Growth media was removed from the cells, replaced by precipitated DNA and incubated at room temperature for 20 minutes. Growth media was then added back to the cells. Following a 4-hour incubation, media was removed and cells were incubated in 0.5 mL of 15% glycerol in HEPES-buffered saline for 2.5 minutes. The cells were then rinsed in HEPES buffered-saline and cultured under normal conditions.

NIH-3T3 cells and myofiber-associated satellite cells were transfected by Lipofectamine 2000. NIH-3T3 cells were grown on 15 cm plates to near confluence. Cells were then transfected using 72 ng DNA and 180 µl Lipofectamine 2000 according to the manufacturers protocol. Myofiber-associated satellite cells cultured in 6-well plates with between 200 and 500 fibers per well and transfected immediately following isolation with 4 µg DNA and 10 µl Lipofectamine 2000 according to the manufacturers protocol.

Reporter Assays

Pathdetect CHOP reporting system (Stratagene) was used to determine p38 MAPK activity (Aguirre-Ghiso et al., 2003). For this assay, MM14 cells were co-transfected with 2.5 µg pFR-Luc reporter vector, 500 ng pFA-CHOP vector and 1 µg CMV-LacZ vector per well. The cells were harvested and luciferase activity was determined 36 hours following transfection.

Luciferase activity was determined by using a Tropix Dual Light assay kit and quantitated with a luminometer (Optocomp I; MGM Instruments, Inc). Luciferase activity values (relative light units) were normalized to β-galactosidase activity values (relative light units) to correct for transfection efficiency. The CMV promoter was chosen to drive the LacZ gene since this promoter exhibits the lowest level of change of all promoters tested (<1.5-fold) between proliferating and differentiated MM14 cell populations.

A muscle differentiation-sensitive reporter containing the firefly luciferase gene driven by a muscle-specific promoter (human α-cardiac actin promoter) (Kudla et al., 1995) was used to determine the extent of MM14 differentiation following transfection. MM14 cells were co-transfected with 1 μg of muscle-specific promoter reporter vector, 1 μg of CMV-LacZ, and different amounts of expression vector or control vector as indicated. Equivalent DNA concentrations were maintained by the addition of pcDNA3 vector (Invitrogen). Cells were harvested and luciferase activity was determined 36 hours following transfection as described above.

MyoD transcriptional activity was determined using a *MyoD*-Gal4 assay. Either MM14 cells or primary satellite cells were co-transfected with 2.5 μg pFR-Luc vector, 500 ng *MyoD*-Gal4 activator construct and 1 μg CMV-LacZ vector. Luciferase activity was determined 36 hours following transfection as described above. In a separate set of control experiments, cells were transfected with Gal4 reporter alone or with either *MyoD*-Gal4, *MyoD*-Gal4 replaced by vector encoding Gal4 DNA binding domain only, or PFR-Luc. In all control experiments luciferase values were indistinguishable from a sample that did not contain cells.

Western Blotting

Transfected NIH-3T3 cells were sorted for mCherry expression by MoFlo XDP Cell Sorter (Beckman Coulture) and transferred to ice cold RIPA lysis buffer. MM14 cells were rinsed and scraped from plate in ice cold RIPA buffer. Samples were then agitated for 30 minutes at 4ºC, centrifuged at 12,000 rpm for 20 minutes at 4ºC and the supernatant was retained. Protein in whole cell lysates was quantified by BCA+ protein assay (Pierce) and equal volumes and amounts of protein (10-20 μg) were resolved in polyacrylamide-SDS gels and transferred to Immobilon-P membrane. Proteins were detected using enhanced chemiluminescence (ECL), using antibodies directed against PKCλ and PKCζ (Santa Cruz) at 1:1000 dilution) or Par-3 (Upstate) at 1:2000. The blocking peptides were also purchased from Santa Cruz Biologicals and used at 10-fold excess by weight according to the manufacturers' instructions. The protein band intensity, normalized to Ponceau staining, was quantified using ImageJ.

Supplemental References

Bader, D., Masaki, T., and Fischman, D.A. (1982). Immunochemical analysis of myosin heavy chain during avian myogenesis in vivo and in vitro. J. Cell Biol. 95, 763–770.

Chen, X., and Macara, I.G. (2005). Par-3 controls tight junction assembly through the Rac exchange factor Tiam1. Nat Cell Biol *7*, 262-69.

Cusella-De Angelis, M.G., Lyons, G., Sonnino, C., De Angelis, L., Vivarelli, E., Farmer, K., Wright, W.E., Molinaro, M., Bouchè, M., Buckingham, M., et al. (1992). MyoD, myogenin independent differentiation of primordial myoblasts in mouse somites. J. Cell Biol. 116, 1243–1255.

Deacon, K., and Blank, J.L. (1997). Characterization of the mitogen-activated protein kinase kinase 4 (MKK4)/c-Jun NH2-terminal kinase 1 and MKK3/p38 pathways regulated by MEK kinases 2 and 3. MEK kinase 3 activates MKK3 but does not cause activation of p38 kinase in vivo. J Biol Chem *272*, 14489-496.

Dérijard, B., Raingeaud, J., Barrett, T., Wu, I.H., Han, J., Ulevitch, R.J., and Davis, R.J. (1995). Independent human MAP-kinase signal transduction pathways defined by MEK and MKK isoforms. Science *267*, 682-85.

Du, Y., Böck, B.C., Schachter, K.A., Chao, M., and Gallo, K.A. (2005). Cdc42 induces activation loop phosphorylation and membrane targeting of mixed lineage kinase 3. J Biol Chem *280*, 42984-993.

Gerwins, P., Blank, J.L., and Johnson, G.L. (1997). Cloning of a novel mitogen-activated protein kinase kinase kinase, MEKK4, that selectively regulates the c-Jun amino terminal kinase pathway. J Biol Chem *272*, 8288-295.

Hirai, S., Katoh, M., Terada, M., Kyriakis, J.M., Zon, L.I., Rana, A., Avruch, J., and Ohno, S. (1997). MST/MLK2, a member of the mixed lineage kinase family, directly phosphorylates and activates SEK1, an activator of c-Jun N-terminal kinase/stress-activated protein kinase. J Biol Chem *272*, 15167-173.

Innocenti, M., Zippel, R., Brambilla, R., and Sturani, E. (1999). CDC25(Mm)/Ras-GRF1 regulates both Ras and Rac signaling pathways. FEBS Lett *460*, 357-362.

Joberty, G., Petersen, C., Gao, L., and Macara, I.G. (2000). The cell-polarity protein Par6 links Par3 and atypical protein kinase C to Cdc42. Nat Cell Biol *2*, 531-39.

Kuang, S., Chargé, S.B., Seale, P., Huh, M., and Rudnicki, M.A. (2006). Distinct roles for Pax7 and Pax3 in adult regenerative myogenesis. J. Cell Biol. 172, 103–113.

Kudla, A.J., John, M.L., Bowen-Pope, D.F., Rainish, B., and Olwin, B.B. (1995). A requirement for fibroblast growth factor in regulation of skeletal muscle growth and differentiation cannot be replaced by activation of platelet-derived growth factor signaling pathways. Mol. Cell. Biol. 15, 3238–3246.

Lambert, J.M., Karnoub, A.E., Graves, L.M., Campbell, S.L., and Der, C.J. (2002). Role of MLK3-mediated activation of p70 S6 kinase in Rac1 transformation. J Biol Chem *277*, 4770-77.

Manser, E., Leung, T., Salihuddin, H., Zhao, Z.S., and Lim, L. (1994). A brain serine/threonine protein kinase activated by Cdc42 and Rac1. Nature *367*, 40-46.

Nagata, K., Puls, A., Futter, C., Aspenstrom, P., Schaefer, E., Nakata, T., Hirokawa, N., and Hall, A. (1998). The MAP kinase kinase kinase MLK2 co-localizes with activated JNK along microtubules and associates with kinesin superfamily motor KIF3. EMBO J *17*, 149-158.

Nishimura, T., Yamaguchi, T., Kato, K., Yoshizawa, M., Nabeshima, Y., Ohno, S., Hoshino, M., and Kaibuchi, K. (2005). PAR-6-PAR-3 mediates Cdc42-induced Rac activation through the Rac GEFs STEF/Tiam1. Nat Cell Biol *7*, 270-77.

Raingeaud, J., Whitmarsh, A.J., Barrett, T., Dérijard, B., and Davis, R.J. (1996). MKK3- and MKK6-regulated gene expression is mediated by the p38 mitogen-activated protein kinase signal transduction pathway. Mol Cell Biol *16*, 1247-255.

Takekawa, M., Posas, F., and Saito, H. (1997). A human homolog of the yeast Ssk2/Ssk22 MAP kinase kinase kinases, MTK1, mediates stress-induced activation of the p38 and JNK pathways. EMBO J *16*, 4973-982.

Uhlik, M.T., Abell, A.N., Johnson, N.L., Sun, W., Cuevas, B.D., Lobel-Rice, K.E., Horne, E.A., Dell'Acqua, M.L., and Johnson, G.L. (2003). Rac-MEKK3-MKK3 scaffolding for p38 MAPK activation during hyperosmotic shock. Nat Cell Biol *5*, 1104-110.

Yamanaka, T., Horikoshi, Y., Suzuki, A., Sugiyama, Y., Kitamura, K., Maniwa, R., Nagai, Y., Yamashita, A., Hirose, T., et al. (2001). PAR-6 regulates aPKC activity in a novel way and mediates cell-cell contact-induced formation of the epithelial junctional complex. Genes Cells *6*, 721-731.

Zhang, S., Han, J., Sells, M.A., Chernoff, J., Knaus, U.G., Ulevitch, R.J., and Bokoch, G.M. (1995). Rho family GTPases regulate p38 mitogen-activated protein kinase through the downstream mediator Pak1. J Biol Chem *270*, 23934-36.